JOURNAL OF VIROLOGY, Apr. 2005, p. 5059–5068 Vol. 79, No. 8
0022-538X/05/$08.00+0 doi:10.1128/JVI.79.8.5059–5068.2005

The Murine Gammaherpesvirus 68 ORF27 Gene Product Contributes to Intercellular Viral Spread

Janet S. May, Jennifer Walker,† Susanna Colaco, and Philip G. Stevenson*

Division of Virology, Department of Pathology, University of Cambridge, Cambridge, United Kingdom

Received 23 November 2004/Accepted 16 January 2005

Herpesviruses remain predominantly cell associated within their hosts, implying that they spread between cells by a mechanism distinct from free virion release. We previously identified the efficient release of murine gammaherpesvirus 68 (MHV-68) virions as a function of the viral gp150 protein. Here we show that the MHV-68 ORF27 gene product, gp48, contributes to the direct spread of viruses from lytically infected to uninfected cells. Monoclonal antibodies to gp48 identified it on infected cell surfaces and in virions. gp48-deficient viruses showed no obvious deficit in virion cell binding, single-cycle replication, or virion release but had reduced lytic propagation between cells. After intranasal infection of mice, ORF27-deficient viruses were impaired predominantly in lytic replication in the lungs. There was a small deficit in latency establishment, but long-term latency appeared normal. Since ORF27 has homologs in both Epstein-Barr virus and Kaposi's sarcoma-associated herpesvirus, it is likely part of a conserved mechanism employed by gammaherpesviruses to disseminate lytically in their hosts.

Epidemic viruses generally rely on high infectivities to transmit infection before immune responses become effective. In contrast, persistent viruses use immune evasion to establish a state of chronic, low-level infectivity. In keeping with this strategy of stealth, persistent viruses generally release virions only in very specific settings and otherwise spread via cell-cell contact.

Herpesviruses are archetypal persistent pathogens. Acute infections are not associated with a detectable viremia, consistent with a predominance of direct, cell-to-cell virus transfer. In herpes simplex virus, this is a function of gE and gI, which are dispensable for lytic replication in vitro but contribute to dissemination in vivo (11). Glycoprotein D of pseudorabies virus, which binds virions to cells, illustrates the converse: it is important for growth in vitro but dispensable for growth in vivo (22). Thus, spread by virion release and spread by cell-cell contact, though clearly overlapping in their requirements for membrane fusion, appear to be separable processes involving distinct attachment proteins. Any therapeutic intervention must therefore encompass these two separate modes of viral spread.

We are interested in the molecular processes that underlie the dissemination of gammaherpesviruses. These viruses lack genetic homologs of alphaherpesvirus gE and gI. The virus-driven proliferation of latently infected lymphocytes plays a central role in host colonization by gammaherpesviruses (8), but lytic replication must still be required for entry into and exit from hosts as well as for viral transit between different cell types. Cell-binding virion proteins have been identified for Epstein-Barr virus (EBV) (6, 32) and Kaposi's sarcoma-associated herpesvirus (KSHV) (2), but the processes by which gammaherpesviruses spread between cells in vivo remain unknown. Moreover, the strict species tropisms of EBV and KSHV make it difficult to use them to identify such functions. Murine gammaherpesvirus 68 (MHV-68) is a related virus of mice (3, 12, 34) that expresses genes homologous to those of EBV and KSHV in a more experimentally accessible setting. We are therefore using MHV-68 to identify how gammaherpesvirus glycoproteins contribute to host colonization.

MHV-68 encodes nine predicted membrane-bound glycoproteins that potentially contribute to cell-to-cell spread. gB, gH, and gL are conserved in all mammalian herpesviruses and are likely to be essential for membrane fusion (9, 23, 25). This would imply that they are also necessary for cell-to-cell spread, but they may not be sufficient in the context of natural infection. gM and gN are also widely conserved in herpesviruses, and gM is an essential protein of MHV-68 (20, 21), but the gM/gN heterodimer functions mainly in virion assembly and egress (7, 17). ORF4 encodes a complement-binding protein (15), and gp150 promotes virion release (10, 30). In addition to these glycoproteins, the predicted multiple membrane-spanning protein encoded by ORF58 may play a role in virion attachment to polarized cells (33). However, the RGD motif implicated in this function for the EBV ORF58 homolog, BMRF2, is not conserved in MHV-68 or KSHV.

The ORF27 and ORF28 gene products of MHV-68 are candidates for playing a role in cell-to-cell viral spread, simply by virtue of encoding putative glycoproteins of unknown function. Both have homologs in KSHV (ORF27 and ORF28) and EBV (BDLF2 and BFLF3). EBV lacking BDLF3 shows enhanced rather than reduced infection of epithelial cells (5), and we have found no obvious replication deficit in MHV-68 lacking its BDLF3 homolog, ORF28 (20a). We therefore characterized the MHV-68 ORF27 gene product and its role in infection. ORF27 was found to encode a glycoprotein, gp48, which is expressed on the surfaces of infected cells and is present in purified virions. ORF27-deficient MHV-68 was

* Corresponding author. Mailing address: Division of Virology, Department of Pathology, University of Cambridge, Tennis Court Road, Cambridge CB2 1QP, United Kingdom. Phone: 44-1223-336921. Fax: 44-1223-336926. E-mail: pgs27@mole.bio.cam.ac.uk.

† Present address: Cambridge Institute for Medical Research, University of Cambridge School of Clinical Medicine, Cambridge CB2 2XY, United Kingdom.

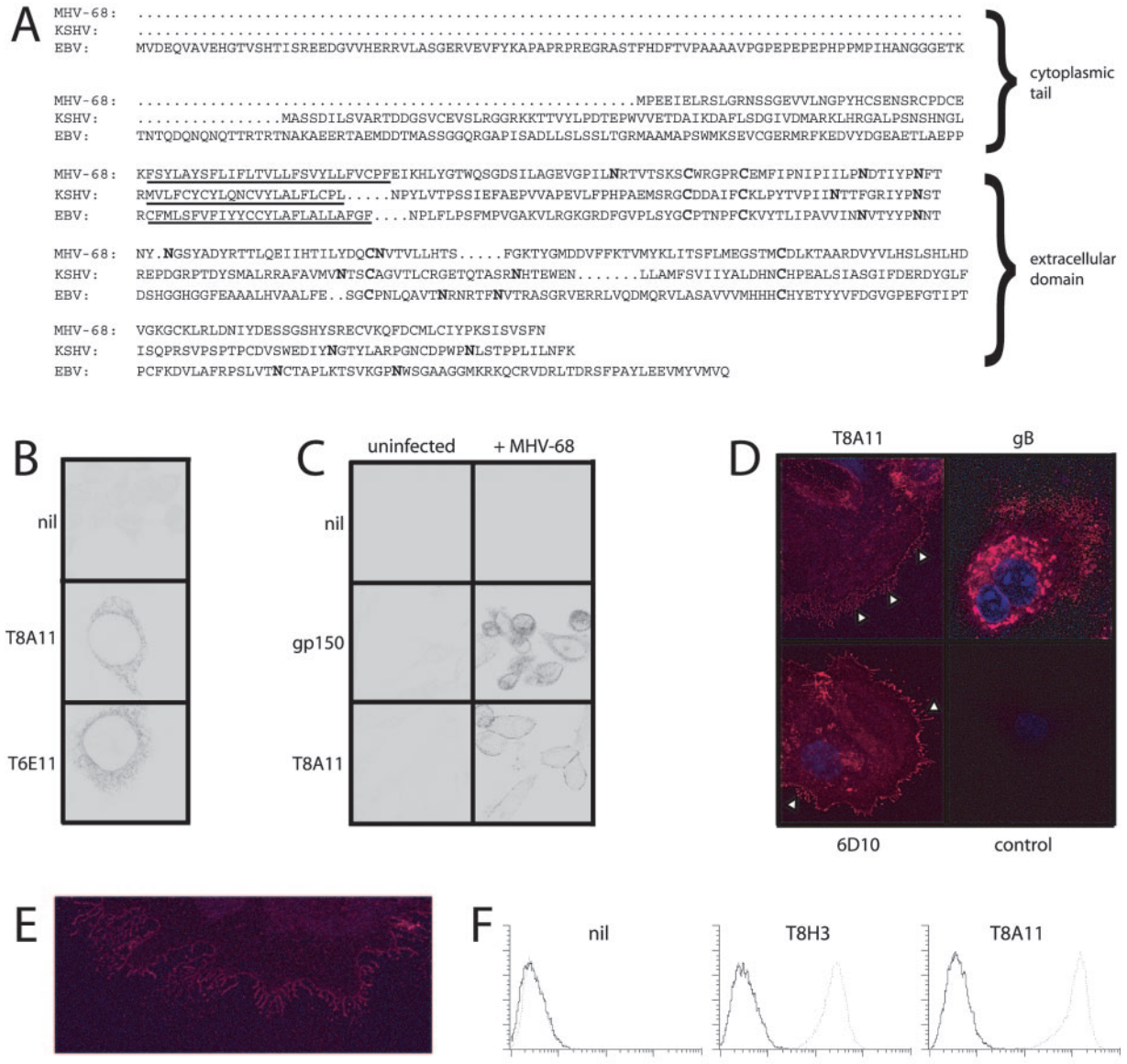

FIG. 1. Identification of the ORF27 gene product on virus-infected cell surfaces. (A) Aligning the MHV-68, KSHV, and EBV ORF27 homologs revealed differences in cytoplasmic tail length but similar arrangements of consensus N-linked glycan attachment sites and extracellular cysteine residues (shown in bold). (B) Perinuclear membrane staining of BHK-21 cells transfected with an ORF27 expression plasmid by the use of MAbs T8A11 and T6E11. Nil, secondary antibody only. There was no staining of untransfected cells. (C) Plasma membrane staining of BHK-21 cells infected with MHV-68 (2 PFU/cell, 18 h) and stained with the T8A11 MAb. gp150 staining with the T4G2 MAb, which was localized mainly on the internal membranes of infected cells, is shown for comparison. (D) The ORF27-specific MAbs T8A11 and 6D10 prominently stained fine cytoplasmic processes (arrowheads) extending from MEFs infected with MHV-68 (2 PFU/cell, 18 h). The staining of MHV-68-infected cells for gB with the T7H9 MAb is shown for comparison. Control, uninfected cells stained with the T8A11 MAb. (E) Higher-magnification image of plasma membrane processes on MHV-68-infected MEFs stained with MAb T8A11. (F) Flow cytometric staining of BHK-21 cells either infected with MHV-68 (2 PFU/cell, 18 h, dotted lines) or left uninfected (solid lines). The cells were stained without fixation or permeabilization. Nil, secondary antibody only.

found to be defective in intercellular viral spread. The ORF27 gene product therefore represents a glycoprotein with homologs in many gammaherpesviruses that, at least in MHV-68, promotes efficient viral spread within the infected host.

MATERIALS AND METHODS

Mice. Female BALB/c and C57BL/6 mice were bred by Harlan UK Ltd. (Bicester, United Kingdom) and housed at the Biological Services Unit of the Cambridge University Department of Pathology. Mice were infected intranasally at 6 to 8 weeks of age with 2×10^4 PFU of virus in a volume of 30 μl, in accordance with Home Office Project License 80/1579.

Cell lines. Baby hamster kidney (BHK-21), NIH 3T3-CRE (29), NS0, and RAW264.7 cells and murine embryonic fibroblasts (MEFs) were grown in Dulbecco's modified Eagle medium (Invitrogen, Paisley, United Kingdom) supplemented with 2 mM glutamine, 100 U of penicillin/ml, 100 μg of streptomycin/ml, and 10% fetal calf serum (PAA Laboratories, Linz, Austria) (complete medium) as previously described. The medium for MEFs was further supplemented with 50 μM 2-mercaptoethanol.

Plasmids. MHV-68 ORF27 (genomic coordinates 45329 to 46093) (34), including EcoRI and XhoI restriction sites introduced by the 5′ and 3′ primers,

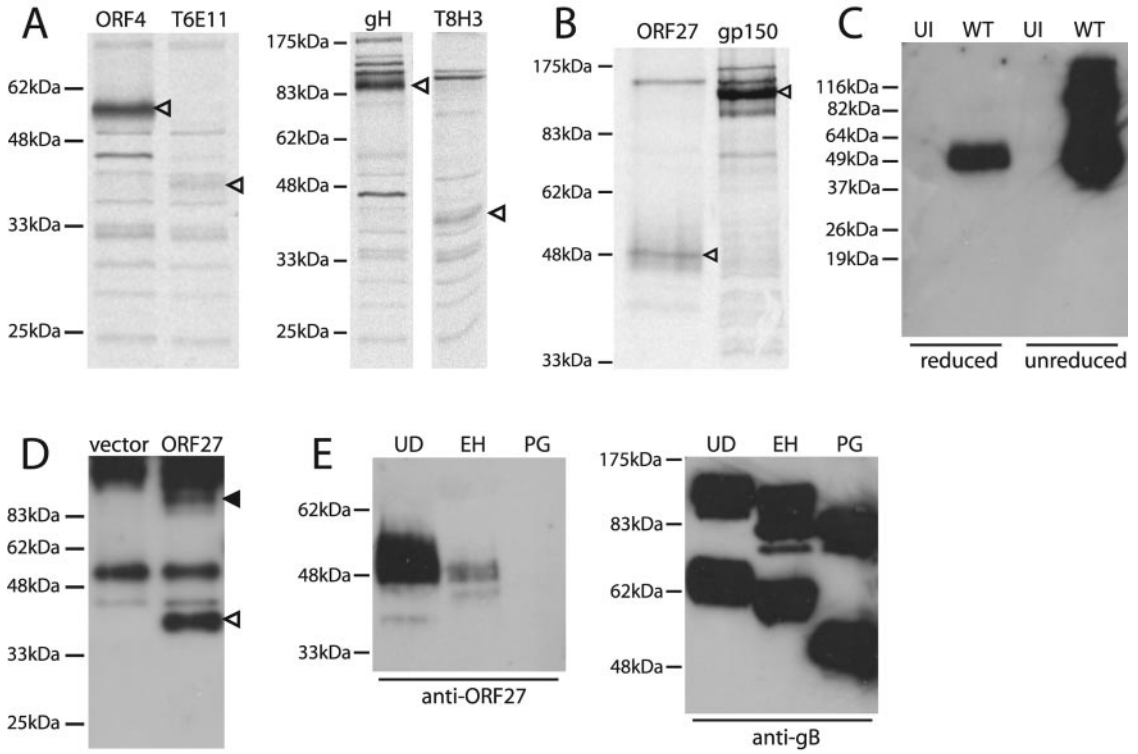

FIG. 2. The mature ORF27 gene product is a 48-kDa glycoprotein. (A) BHK-21 cells were infected with MHV-68 (2 PFU/cell), and 18 h later, were labeled with [^{35}S]cysteine-methionine for 1 h. ORF27 was then immunoprecipitated with the T6E11 or T8H3 MAb. Immunoprecipitations with the ORF4-specific MAb T3B8 and the gH-specific MAb 2G2 are shown for comparison. Arrowheads indicate specific precipitated bands. (B) For this experiment, the label was chased overnight with an excess of unlabeled cysteine-methionine. Virions were then recovered from cell-free supernatants by ultracentrifugation. ORF27 was immunoprecipitated from virion lysates with the T8A11 MAb. The immunoprecipitation of gp150 with MAb T4G2 is shown for comparison. Arrowheads indicate specific bands. (C) Lysates of purified MHV-68 virions (WT) or uninfected (UI) BHK-21 cells were immunoblotted with the 6D10 MAb. The samples were reduced or not with 5% 2-mercaptoethanol before electrophoresis, as indicated. (D) 293T cells were transfected with an ORF27 expression plasmid or an empty vector. Forty-eight hours later, the samples were immunoprecipitated with the T8A11 MAb and then immunoblotted with the T8H3 MAb, as the ORF27 protein was difficult to identify simply by immunoblotting transfected cell lysates. The open arrowhead indicates the major specific band. There was also a possible higher-molecular-mass, ORF27-specific band (filled arrowhead), but this was difficult to distinguish from the precipitating MAb. The samples were unreduced, so even though the band at 55 kDa corresponds to the IgG heavy chain, the bulk of the immunoglobulin ran intact at higher molecular masses. (E) Infected cell lysates were reduced, denatured, and then either left undigested (UD), digested with endoglycosidase H (EH), or digested with protein *N*-glycanase (PG). The samples were then immunoblotted with the T8H3 MAb (a similar pattern was observed with the 6D10 MAb). Immunoblotting of the same samples with the gB-specific MAb T7H9 provided a control of protein integrity.

respectively, was amplified from viral DNA by PCR (Hi-Fidelity kit; Roche Diagnostics, Lewes, United Kingdom) and cloned into the EcoRI and XhoI sites of pMSCV-IRES-NEO (28). The empty vector was used as a control. Plasmids were transfected into BHK-21 cells by the use of Fugene-6 (Roche Diagnostics) according to the manufacturer's instructions.

Viral mutagenesis. We generated two nonoverlapping ORF27 mutants by using an MHV-68 genomic bacterial artificial chromosome (BAC) (1). First, a kanamycin resistance gene flanked by Flp recombinase target (FRT) sites was amplified by PCR from BsaI-linearized pCP15 by the use of primers with 50-bp 5′ extensions corresponding to genomic coordinates 45311 to 45360 and 45440 to 45391. The purified PCR product was electroporated into *Escherichia coli* JC8679 containing the MHV-68 BAC and recombined into the ORF27 coding sequence by the constitutive RecE/T activity of this bacterium. Recombinant BACs were isolated from chloramphenicol- and kanamycin-resistant colonies and transformed into *E. coli* DH10B. The bacteria were then transformed with a temperature-sensitive Flp recombinase expression plasmid, pCP20, to excise the kanamycin resistance gene. This left 166 bp of foreign sequence in the BAC, comprising a single FRT site, in-frame stop codons, and short, flanking plasmid sequences, in place of 30 bp of ORF27. The *E. coli* DH10B cells were cured of pCP20 by growth at 43°C. Correct mutagenesis was confirmed by restriction enzyme mapping of the BAC DNA. For construction of a revertant virus, the BamHI-C genomic clone (genomic coordinates 42401 to 49938) (12) was subcloned from pUC9 into the pST76K-SR shuttle vector and recombined into the mutant BAC by transient RecA expression according to established protocols (1). ORF27 repair was confirmed by digestion of the BAC DNA with EcoRI. An independent ORF27 mutant was made by inserting an oligonucleotide encoding multiple stop codons into a ScaI site in the ORF27 coding sequence. The ScaI site in pACYC177 (New England Biolabs, Hitchin, United Kingdom) was removed by digestion with ScaI and HincII and ligation of the linearized plasmid back to itself. The BamHI-C genomic fragment was subcloned into the modified pACYC177 plasmid, digested with ScaI, which cuts at genomic coordinate 45480, and treated with shrimp alkaline phosphatase (Roche Diagnostics). A palindromic oligonucleotide containing a diagnostic EcoRI restriction site and stop codons in all reading frames (5′-CTAGCTAGCTAGAATTCTAGCTAGCTA G-3′) was heated, annealed, phosphorylated with polynucleotide kinase (New England Biolabs), and ligated into the ScaI site of ORF27. The mutant BamHI-C fragment was then subcloned into the pST76K-SR shuttle vector and recombined into the mutant BAC by transient RecA expression as described above. All BACs were reconstituted into infectious viruses by transfecting BAC DNAs into BHK-21 cells by the use of Fugene-6. The loxP-flanked BAC-GFP cassette was removed by passaging the virus through NIH 3T3-CRE cells.

Virus growth and titration. All virus stocks were grown and titrated in BHK-21 cells (10). Infected cells were harvested when >50% of them showed cytopathic effects. After sonication, cell debris was pelleted by low-speed centrifugation (1,000 × *g*, 3 min) and discarded. Virions were then pelleted by high-speed centrifugation (38,000 × *g*, 90 min), resuspended in complete medium, and

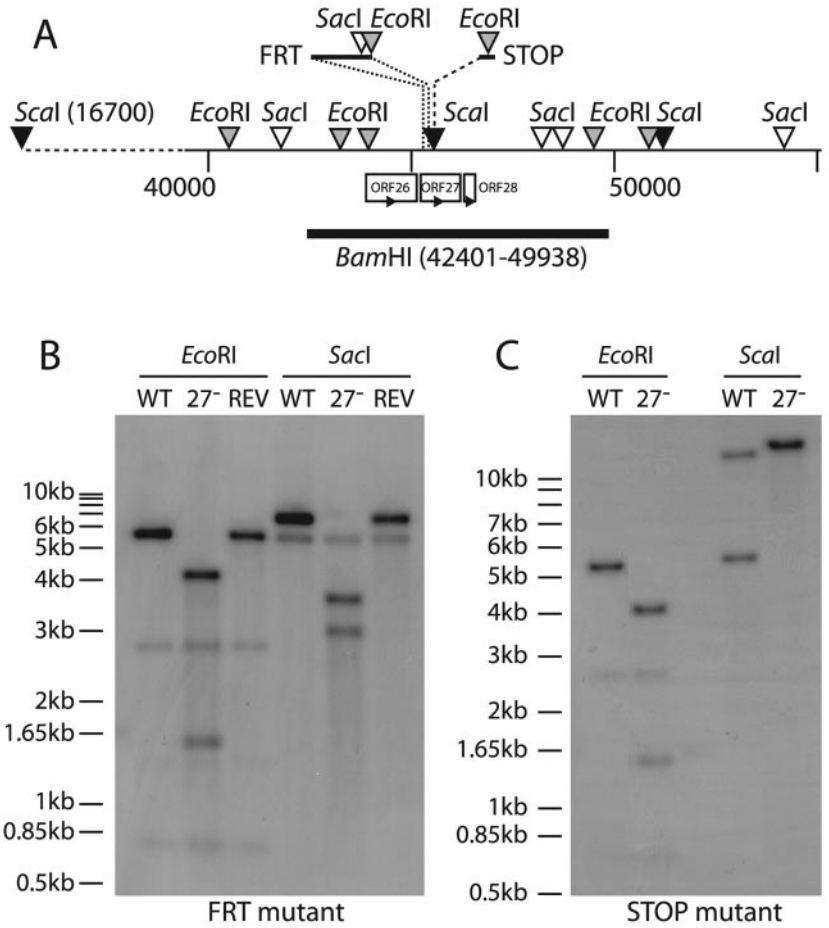

FIG. 3. Disruption of ORF27 in the MHV-68 genome. (A) The sites of ORF27 mutagenesis are shown, as are relevant genomic and introduced restriction sites. Both mutations were located near the 5′ end of ORF27, downstream of the 3′ end of ORF26, and well upstream of the 5′ end of ORF28. The positions and orientations of the neighboring ORFs are shown. (B) The BamHI-C genomic fragment shown in panel A was used as a probe template for Southern blotting of viral DNA derived from the wild-type virus (WT), the ORF27$^-$ FRT mutant (27$^-$), or its revertant (REV). The predicted fragments for WT viral DNA were 2,703, 744, 5,611, and 1,342 bp for EcoRI (the 1,342-bp band is very faint due to limited overlap with the probe) and 6,531, 372, and 5,553 bp for SacI. With the FRT mutation, the 5,611-bp EcoRI band was cut into 4,150- and 1,546-bp bands, and the 6,531-bp SacI band was cut into 2,941- and 3,675-bp bands. (C) Southern blot of viral DNAs derived from the wild-type virus (WT) and the ORF27$^-$ STOP mutant (27$^-$), again with the BamHI-C genomic fragment as the probe template. With the STOP mutation, the 5,611-bp EcoRI band was cut into 4,075- and 1,536-bp bands. The predicted bands for ScaI digestion of the WT viral DNA were 28,780 and 5,721 bp. Insertion of the STOP oligonucleotide disrupted the ScaI site at genomic coordinate 45480 to give a single band of 34,501 bp.

stored in aliquots at −70°C. For the preparation of purified virions, virus stocks were layered over 5 to 15% Ficoll gradients and then centrifuged (30,000 × *g*, 90 min). The virions were recovered as a distinct band, resuspended in phosphate-buffered saline (PBS), pelleted (30,000 × *g*, 90 min), sonicated, and stored at −70°C. For titrations of infectious viruses in the lungs, the lungs were homogenized in complete medium, frozen, thawed, and sonicated. Tissue debris was pelleted by a brief centrifugation step (1,000 × *g*, 1 min). Infectious viruses in homogenate supernatants were measured by a plaque assay with MEFs (10). Monolayers were fixed in 10% formaldehyde after 6 days and stained with 0.1% toluidine blue. Plaques were counted with a plate microscope. Latent viruses in spleens were measured by explant culturing of single-spleen-cell suspensions on MEF monolayers. These cultures were fixed and stained after 7 days.

Southern blotting. DNAs were extracted from virus stocks by alkaline lysis (19), digested with restriction endonucleases, electrophoresed in 0.8% agarose gels, and transferred to positively charged nylon membranes (Roche Diagnostics). A [^{32}P]dCTP-labeled probe (APBiotech, Little Chalfont, United Kingdom) was generated by random primer extension (Nonaprimer kit; Qbiogene, Bingham, United Kingdom) according to the manufacturer's instructions. Membranes were hybridized with the probe (65°C, 18 h), washed to a stringency of 0.2% SSC (1× SSC is 0.15 M NaCl plus 0.015 M sodium citrate)–0.1% sodium dodecyl sulfate (SDS), and exposed to X-ray film.

Immunoblotting and immunoprecipitation. Monoclonal antibodies (MAbs) specific for ORF27 were generated by fusing spleen cells of MHV-68-immune mice with NS0 cells (16). We derived the following four ORF27-specific MAbs: T6E11 (immunoglobulin G2a [IgG2a]), T8A11 (IgG2a), T8H3 (IgG1), and 6D10 (IgG2a). MAbs against gB (T7H9) (18), gp150 (T4G2), and ORF4 (T3B8) (10) were used as controls. For immunoblotting, samples were lysed on ice for 30 min in a mixture containing 1% Triton X-100, 50 mM Tris-Cl (pH 7.4), 150 mM NaCl, 5 mM EDTA, 1 mM phenylmethylsulfonyl fluoride, and Complete protease inhibitors (Roche Diagnostics). Insoluble debris was removed by centrifugation (13,000 × *g*, 15 min). Cleared lysates were then heated (50°C, 15 min) in Laemmli's buffer, with or without 5% 2-mercaptoethanol, resolved by SDS-polyacrylamide gel electrophoresis, and transferred to polyvinylidene difluoride membranes (Perbio Science, Tattenhall, United Kingdom). ORF27-specific immunoblotting was performed with the 6D10 or T8H3 MAb, followed by a horseradish peroxidase-conjugated rabbit anti-mouse IgG polyclonal Ab (Dako Corporation, Ely, United Kingdom) and ECL substrate development (APBiotech). For immune precipitation, MHV-68-infected cells (5 PFU/cell, 18 h) were labeled for 1 h with [^{35}S]cysteine-methionine (Perkin-Elmer Life Sciences, Cambridge, United Kingdom) (4). When indicated, the label was chased by the addition of 2 mM unlabeled cysteine-methionine. Labeled cells were lysed as for immunoblotting. Lysates

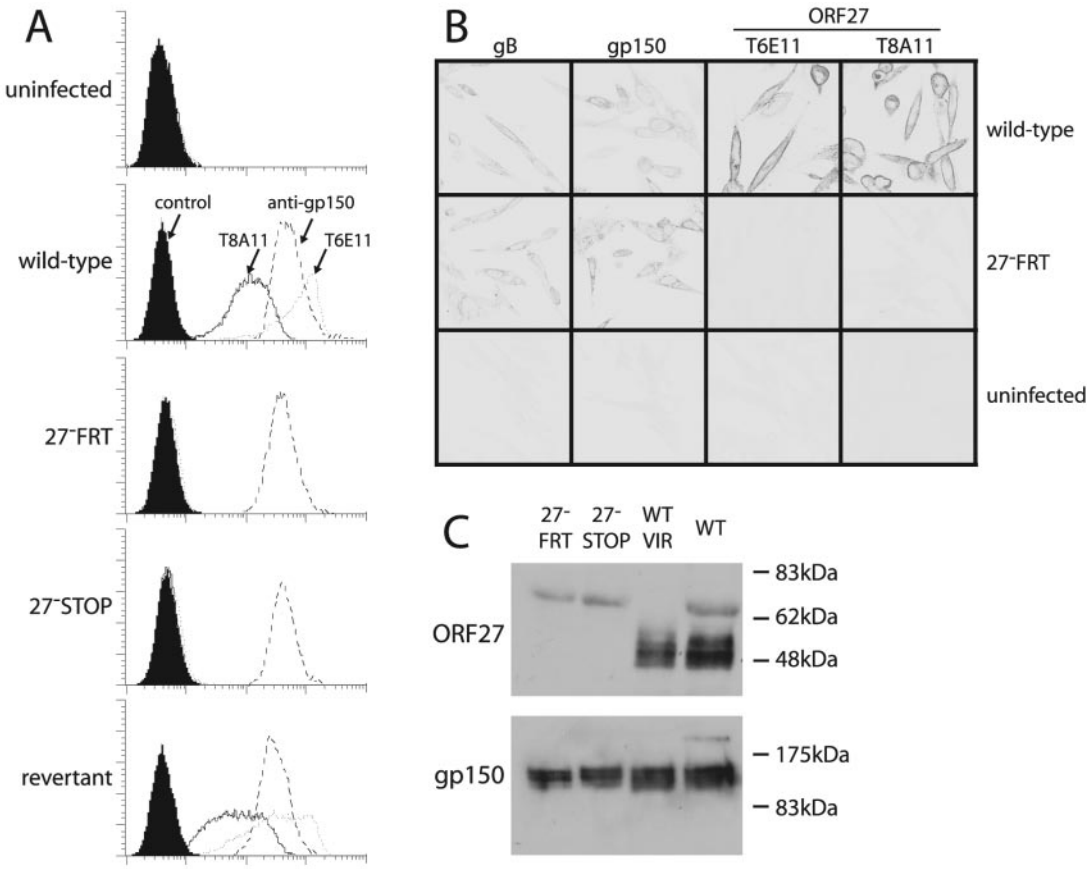

FIG. 4. Absence of gp48 expression after disruption of ORF27. (A) BHK-21 cells were infected (18 h, 2 PFU/cell) as indicated and assayed for cell surface gp48 expression by flow cytometric staining with the MAbs T8A11 and T6E11. The gp150-specific MAb T4G2 was used as a positive control. (B) BHK-21 cells were infected as described for panel A, fixed in methanol, permeabilized with 0.1% Tween 20, and stained as indicated. The gB-specific MAb T7H9 and the gp150-specific MAb T4G2 were used as positive controls. (C) Wild-type (WT) and mutant (27^- FRT and 27^- STOP) virus stocks were lysed in Laemmli's buffer and immunoblotted for gp48 with the T8H3 MAb or for gp150 with the T4G2 MAb. The 65-kDa band corresponds to bovine albumin (virus stocks were resuspended in medium with 10% fetal calf serum) and was absent from density gradient-purified virions (WT VIR), which were resuspended in PBS.

cleared of debris were further cleared by incubation with protein A-Sepharose (AP Biotech) and then immunoprecipitated with the T8A11 MAb followed by protein A-Sepharose (Sigma Chemical Co., Poole, United Kingdom). Sepharose beads with bound antibody were washed five times in lysis buffer. Samples were dissociated (50°C, 15 min) in Laemmli's buffer, resolved by SDS-polyacrylamide gel electrophoresis, and exposed to X-ray film.

Immunofluorescence. BHK-21 cells or MEFs were either transfected with an ORF27 expression plasmid (48 h) or infected with MHV-68 (18 h). The cells were then washed in PBS, fixed in methanol (−20°C, 5 min), and blocked for 30 min in PBS–10% fetal calf serum–0.1% Tween. For monoclonal antibody staining, hybridoma supernatants were diluted 1/2 in PBS–0.1% Tween and incubated for 1 h at 4°C. Detection was done with Alexa 594-coupled goat anti-mouse IgG (1 h, 4°C). The cells were washed three times in PBS–0.1% Tween 20 after each antibody incubation. For some experiments, nuclei were counterstained with DRAQ-5. Fluorescence was visualized with a Leica confocal microscope.

Flow cytometry. Cells infected with green fluorescent protein-positive (GFP^+) viruses were washed in PBS and analyzed directly for green channel fluorescence. For specific staining, cells were incubated for 30 min on ice alone and then for 1 h on ice with the T8A11, T6E11, T8H3 (all anti-gp48), T7H9 (anti-gB), or T4G2 (anti-gp150) MAb, washed twice, and incubated with a fluorescein isothiocyanate-conjugated rabbit anti-mouse IgG polyclonal Ab (Dako Corporation). After being washed twice, the cells were analyzed on a FACSCalibur cytometer by the use of Cellquest software (Becton-Dickinson, Oxford, United Kingdom). Graphs were plotted with FCSPress, v. 1.3.

RESULTS

Identification of ORF27 gene product. MHV-68 ORF27 is predicted to encode a type II transmembrane protein with multiple N-linked glycosylation sites (Fig. 1A). The sequence conservation between MHV-68 ORF27 and its positional homologs in EBV (BDLF2) and KSHV (ORF27) is relatively low. However, all three proteins share the same basic form, with positionally conserved cysteine residues and the same potential for carrying multiple N-linked glycans. A large panel of MHV-68-specific MAbs was screened for reactivity against cells transfected with ORF27. We identified several MAbs that stained internal membranes of permeabilized, transfected cells, and some examples are shown in Fig. 1B. None of these MAbs stained the plasma membranes of transfected cells, and unfixed cells transfected with ORF27 showed no staining by flow cytometry (data not shown). However, the same MAbs stained the plasma membranes rather than internal membranes of virus-infected cells (Fig. 1C). ORF27 staining was particularly visible on fine membrane extensions reaching out from infected cell surfaces, in contrast for example, to gB (Fig. 1D and E). Flow cytometry of nonpermeabilized

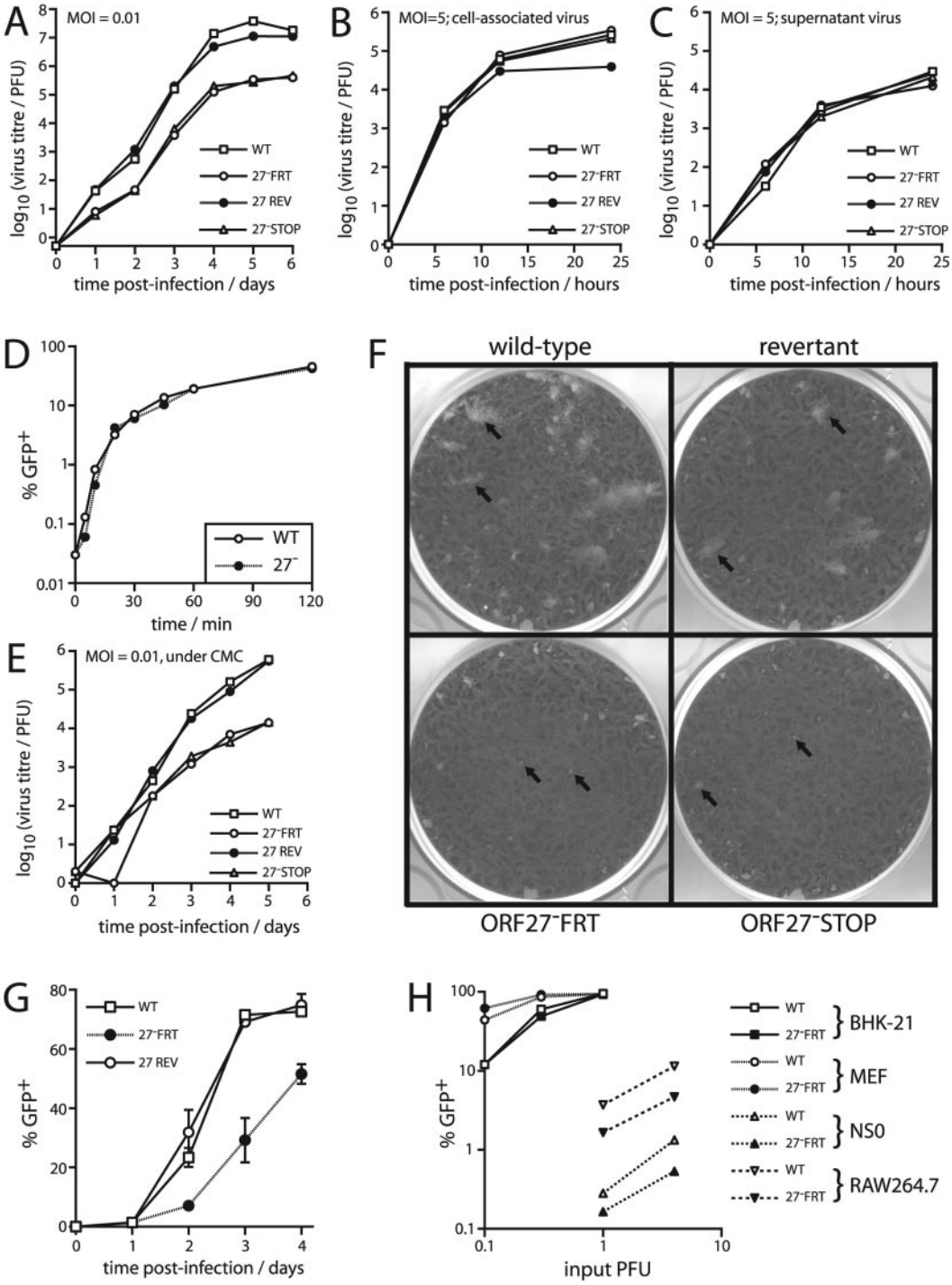

FIG. 5. ORF27 mutant viruses showed impaired low-multiplicity growth in BHK-21 cells. (A) BHK-21 cells were infected at a low multiplicity (0.01 PFU/cell) with ORF27$^+$ (WT and REV) and ORF27$^-$ (FRT and STOP) viruses as indicated. The amounts of infectious virus in cultures were then determined by a plaque assay at the indicated times. Data for one of three equivalent experiments are shown. (B) BHK-21 cells were infected at a high multiplicity (5 PFU/cell) for 2 h at 37°C. The input virus was removed by acid washing, and the infectious virus associated with the cells was measured by a plaque assay as described for panel A. (C) After high-multiplicity infection and acid washing, the amount of infectious virus released into cell-free supernatants over time was measured by a plaque assay. (D) BHK-21 cells were exposed to the GFP$^+$ wild-type (WT) or ORF27$^-$ FRT (27$^-$) virus (1 PFU/cell) at 37°C for the indicated times. The cells were then acid-washed and fed with new medium. Sixteen hours later, the proportion of GFP$^+$ cells was determined by flow cytometry. GFP expression occurred by virtue of retaining the loxP-flanked BAC cassette at the left end of the viral genome. (E) BHK-21 cells were infected at a low multiplicity as described for panel A but were then cultured in medium with 0.6% carboxymethylcellulose (CMC) to prevent the spread of virions throughout the culture medium. (F) BHK-21 monolayers were infected with the indicated viruses and cultured under 0.6% carboxymethylcellulose. The arrows show example plaques. At the dilutions shown, there were larger plaque numbers on the monolayers infected with the ORF27 mutant viruses, but the plaques were smaller. (G) BHK-21 cells were infected with the GFP$^+$ wild-type (WT), ORF27-deficient (27$^-$ FRT), or revertant (27 REV) virus as indicated, at a multiplicity of 0.01

infected cells confirmed that ORF27 was present on the exterior surface of the plasma membrane (Fig. 1F). Thus, ORF27 requires other viral proteins to reach the cell surface, but in infected cells seems to accumulate specifically at the cell surface.

ORF27 encodes gp48. The immunoprecipitation of metabolically labeled, MHV-68-infected cell lysates with ORF27-specific MAbs identified a 40-kDa protein (Fig. 2A). We also pulse-labeled infected cells with [^{35}S]cysteine-methionine and chased the label overnight before recovering virions from cell-free supernatants by ultracentrifugation. ORF27-specific MAbs then immunoprecipitated a 48-kDa protein from the pelleted virions (Fig. 2B). The ORF27 gene product was therefore a virion protein that was processed from a 40-kDa to a 48-kDa form before leaving the cell. We confirmed the presence of the ORF27 gene product in virions by immunoblotting lysates of virions that had been purified through density gradients (Fig. 2C). This identified a 48-kDa band for reduced samples and 48- and 96-kDa bands for unreduced samples. The ORF27 gene product in the virion was therefore disulfide linked in part, probably as a homodimer but possibly as a heterodimer with another viral protein.

In transfected cells, ORF27 remained in its 40-kDa form (Fig. 2D), consistent with its being retained in the endoplasmic reticulum in the absence of other viral proteins (Fig. 1B), rather than being processed to its mature form. The most likely explanation for the increase in size of the ORF27 gene product during maturation in virus-infected cells was that it became more heavily glycosylated. Digesting virion lysates with endoglycosidase H or protein *N*-glycanase made the 48-kDa band more difficult to detect with the ORF27-specific MAbs (Fig. 2E), implying that their cognate epitopes were dependent on N-linked glycans. The fact that endoglycosidase H diminished the intensity of the 48-kDa band argued that a significant fraction of the ORF27 gene product in virions retained at least some high-mannose or hybrid N-linked glycans.

Generation of ORF27-deficient MHV-68. We constructed two nonoverlapping MHV-68 ORF27 mutants (Fig. 3A). In the 27$^-$ FRT mutant, 30 bp near the 5′ end of ORF27 were replaced with a 166-bp insert that introduced stop codons before the putative ORF27 transmembrane domain plus diagnostic EcoRI and SacI restriction sites. In the 27$^-$ STOP mutant, an oligonucleotide was inserted slightly further downstream, again introducing premature stop codons into the ORF27 coding sequence (plus a diagnostic EcoRI site) to prevent the expression of its extracellular domain. Southern blots of the viral DNAs confirmed the predicted genomic structures of each mutant plus a revertant of the ORF27$^-$ FRT mutant (Fig. 3B and C). Correct mutagenesis was further confirmed by sequencing across the mutation sites (data not shown).

Neither ORF27 mutant expressed detectable gp48 at the cell surface, whereas the revertant virus did (Fig. 4A). Also, the immunofluorescence of fixed cells showed no sign of gp48 expression when ORF27 was disrupted (Fig. 4B), and gp48 was undetectable by immunoblotting lysates of cells infected with ORF27-deficient viruses (Fig. 4C).

Impaired dissemination of ORF27-deficient MHV-68 in vitro. Both the STOP and the FRT ORF27$^-$ mutant viruses showed impaired growth in BHK-21 cell monolayers after low-multiplicity infections (Fig. 5A). There was no growth deficit after high-multiplicity infections (Fig. 5B), suggesting a problem with spread between infected cells rather than with single-cycle replication. The release of virions appeared to be normal (Fig. 5C). Also, there was little or no defect in the rate of entry of ORF27-deficient virions into BHK-21 cells (Fig. 5D). These data implied a specific reduction in direct intercellular viral spread.

The relative contributions to in vitro MHV-68 growth of virion release and cell-to-cell spread are unknown. In order to reduce the spread of infection by virion release, we cultured BHK-21 cell monolayers that had been infected at a low multiplicity under a viscous medium (0.6% carboxymethylcellulose) (Fig. 5E). The growth defect remained, which argued against the ORF27-associated deficit being due to a problem with the dissemination of cell-free virions. A notable feature of growth under carboxymethylcellulose was that the ORF27 mutants formed much smaller plaques than wild-type or revertant viruses (Fig. 5F). This was consistent with gp48 contributing to the efficient spread of infection between adjacent cells. ORF27-deficient MHV-68 also showed impaired spread when cultured in the presence of neutralizing antibody (Fig. 5G).

It is possible that gp48 does contribute to the infectivity of virions in some settings. Despite a normal infection of fibroblasts, ORF27-deficient MHV-68 showed a two- to fourfold reduction in infection of RAW264.7 macrophages and NS0 myeloma cells (Fig. 5H). Wild-type MHV-68 virions infect both of these cell lines rather poorly, perhaps because they are relatively deficient in cell surface glycosaminoglycans (10). Thus, when infection was suboptimal, some role for gp48 was apparent, separate from its contribution to cell-to-cell spread in fibroblasts.

Impaired dissemination of ORF27-deficient MHV-68 in vivo. After intranasal infections of BALB/c mice, the ORF27$^-$ FRT mutant showed somewhat reduced replication compared to wild-type MHV-68. The deficit was largest for acute lytic replication in the lungs (Fig. 6A, day 6). There was also some reduction in latent virus in the spleen (Fig. 6B), which may have reflected in part the reduced lytic replication in infected lungs, since the level of lytic replication generally determines how much virus is initially seeded in the lymphoid tissue (8, 27).

Intranasal infections of C57BL/6J mice reproduced the lytic replication deficit observed with BALB/c mice (Fig. 6C). The ORF27$^-$ STOP mutant also showed a replication deficit, whereas the revertant of the ORF27$^-$ FRT mutant grew normally. Thus, the growth deficit was specifically due to ORF27

PFU/cell. Replicate cultures were then maintained in medium supplemented with 2% serum pooled from MHV-68-immune mice. At the time points indicated, GFP expression in sample cultures was determined by flow cytometry of trypsinized cells. Each point shows the mean ± standard deviation of triplicate cultures. (H) BHK-21 cells, MEFs, NS0 myeloma cells, and RAW264.7 macrophages were infected with the GFP$^+$ wild-type (WT) or ORF27-deficient (27$^-$ FRT) virus, as indicated. Eighteen hours later, the cells were analyzed for GFP expression by flow cytometry. PFU titers of virus stocks were determined on BHK-21 cells. The data shown are representative of three independent experiments.

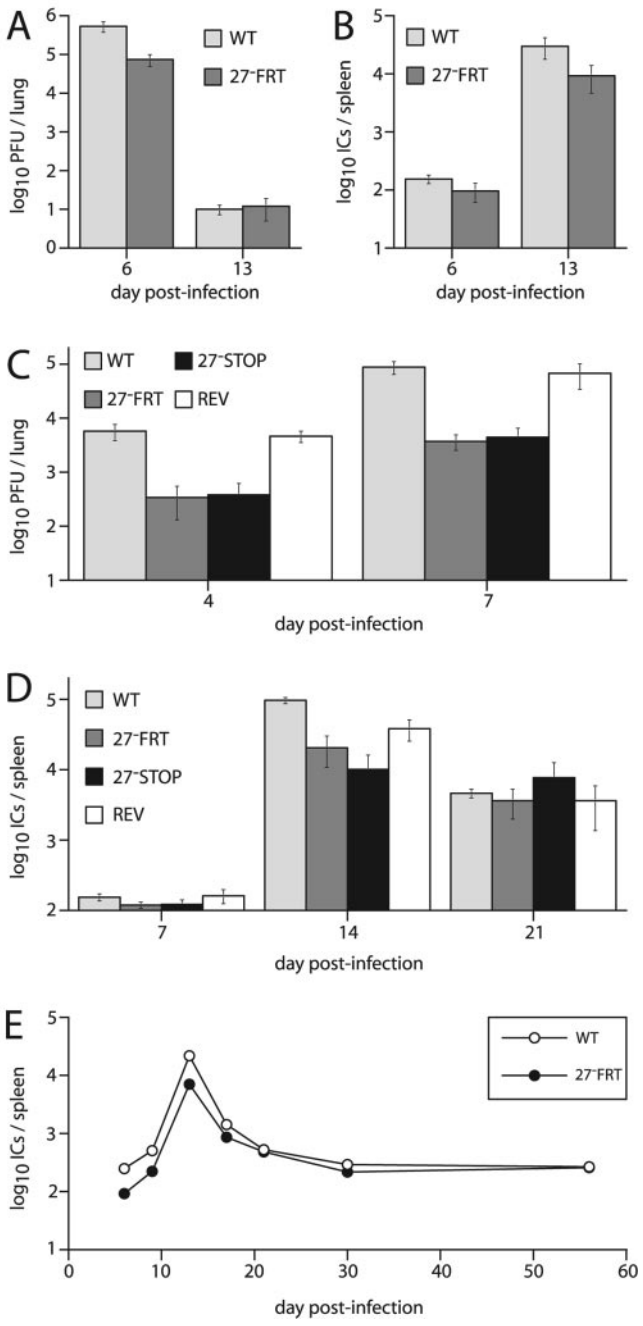

FIG. 6. Growth of ORF27 mutant viruses in vivo. (A) BALB/c mice were infected intranasally (2×10^4 PFU/mouse) with the wild-type (WT) or ORF27-deficient (27^- FRT) virus. Infectious viruses in the lungs were measured by a plaque assay. Means ± standard errors of the means (SEM) of five mice per group are shown. The reduction in titer with the ORF27$^-$ FRT virus on day 6 was significant by Student's *t* test ($P < 0.03$). (B) Latent viruses in the spleens of the same mice that were used for panel A were measured by an infectious center assay. Means ± SEM of five mice per group are shown. Although the 27^- FRT titers were lower than those of the WT, the difference did not reach statistical significance in this experiment ($P = 0.15$). (C) C57BL/6J mice were infected intranasally (2×10^4 PFU/mouse) with ORF27$^+$ (WT and REV) or ORF27$^-$ (STOP and FRT) viruses as indicated. Infectious viruses in lung homogenates were measured by a plaque assay at the indicated times. Means ± SEM of five mice per group are shown. Mutant virus titers were significantly lower than WT titers ($P < 0.03$), whereas the revertant titers (REV) were equivalent to WT titers ($P = 0.7$). (D) Latent viruses in the spleens of mice equivalent to those used for panel C were measured by an infectious center assay. Means ± SEM of five mice per group are shown. There was a significant reduction in the titers of the ORF27 mutants compared to the WT on day 14 after infection ($P < 0.001$) but not between the 27^- FRT mutant and its revertant (REV). There was no significant difference between any of the groups at the other times. (E) BALB/c mice were infected intranasally (2×10^4 PFU/mouse) with the wild-type (WT) or ORF27-deficient (27^- FRT) virus. Latent viruses in spleens were measured by an infectious center assay. Means ± SEM of five mice per group are shown, although the SEM error bars are smaller than the data points. The reduction in latent virus with the 27^- FRT mutant was significant at days 6, 9, 13, and 17 postinfection ($P < 0.03$), but not at later times.

disruption. C57BL/6J mice also showed some reduction in peak levels of latency (day 14), but by day 21 after infection, the reactivatable latent virus titers were equivalent for ORF27$^+$ and ORF27$^-$ viruses (Fig. 6D). A longitudinal analysis of the ORF27$^-$ FRT mutant in BALB/c mice showed a similar pattern (Fig. 6E): the infectious-center titers of the mutant virus were initially lower but converged with those of the wild-type virus by 21 days postinfection. In summary, it is possible that a lack of ORF27 led to a subtle latency deficit in lymphoid tissue, but the major phenotype of the knockout viruses was reduced lytic spread in infected lungs.

DISCUSSION

MHV-68 ORF27 was found to encode a 48-kDa glycoprotein expressed on the surfaces of infected cells. The disruption of ORF27 impaired cell-to-cell viral spread. Since ORF27 is conserved among gammaherpesviruses, it may be part of a mechanism by which these viruses spread between cells in the infected host, analogous to that of alphaherpesvirus gE and gI. The phenotype of ORF27-deficient MHV-68 contrasted with that of M7-deficient MHV-68 (10). The M7 gene product, gp150, is required for efficient virion release from infected fibroblasts, and M7-deficient mutants form normally sized plaques but fail to disseminate widely in vitro (10). ORF27-deficient mutants released virus normally but formed small plaques. These two accessory viral glycoproteins are therefore components of distinct exit pathways from the infected cell, whereby virions can either be released into the extracellular space or be transferred directly to adjacent cells.

As nonmotile parasites, viruses face a fundamental problem in transport from established sites of infection to new cells and new hosts. A general solution to this problem has been for viruses to exploit physiological cellular pathways of mobility and communication (14). Virion release efficiently spreads infection across in vitro fibroblast monolayers, on which the culture medium provides a substantial fluid-filled space for diffusion and convection currents. However, such spaces are rare in vivo, except at mucosal surfaces. Tissue boundaries and the close packing of cells normally limit the dissemination of cell-free virions. For example, neurotropic influenza virus spreads slowly through the brain substance but explosively when it reaches the cerebrospinal fluid (26).

Viruses that disseminate beyond epithelial surfaces have adapted to the anatomical constraints on virion release by evolving mechanisms of direct cell-to-cell spread. The ex-

ploitation of normal cellular functions then allows more efficient virion dissemination than simple diffusion. Such mechanisms are well defined for poxviruses, which use actin polymerization to extend long, virion-laden processes from infected cells (24). MHV-68 infection also induces cellular processes, particularly on macrophages (P. G. Stevenson, unpublished data), and the presence of gp48 on small processes extending from infected MEFs (Fig. 1D) was consistent with a role in efficiently propagating infection between neighboring cells. Growth under a viscous medium places an emphasis on the direct cell-to-cell spread of infection, and under this condition, ORF27-deficient MHV-68 formed only small plaques (Fig. 5F). The corresponding in vivo growth deficit (Fig. 6C) contrasted with the fairly normal in vivo growth of MHV-68 M7 mutants (10).

Despite little or no defect in fibroblast entry, ORF27-deficient virions showed a two- to fourfold reduction in NS0 and RAW264.7 cell infections (Fig. 5H). gp48 may therefore function as an accessory factor in the adhesion or penetration of some nonepithelial cell types in addition to its role in viral spread between epithelial cells. However, gp48 was clearly inessential for viral entry into the B-cell compartment (Fig. 6). The entry of MHV-68 virions into cells with low levels of cell surface glycosaminoglycans, including B cells and macrophages, is inefficient (10), and how MHV-68 normally colonizes these cells types in vivo (13, 31, 35) is unclear. Thus, any role for ORF27 must remain speculative.

Outline functions have now been defined for most of the MHV-68 glycoproteins. The overall picture fits that of other herpesviruses. gB and gH are both essential proteins (21) consistent with a fusion function that probably also incorporates gL. MHV-68 gB is a virion protein (18) that binds to fibroblasts as a soluble Fc fusion protein (Stevenson, unpublished data), suggesting that, like KSHV gB, it has an additional role in virion attachment. The gM/gN complex is also essential (20). A set of accessory glycoproteins supplements these core components. The ORF4 complement control protein, perhaps not surprisingly, functions mainly in immune evasion (15). The virion release function of gp150 is presumably important for MHV-68 transmission. The possibility that gp150 is also important for MHV-68 latency (30) is doubtful. This claim was based on a single mutant with a large genomic deletion, whereas two mutants with more subtle disruptions of the gp150 coding sequence showed no such deficit (10).

In this study, we have shown that gp48 enhances the intercellular spread of infection. There may also be a role for the MHV-68 BMRF2 homolog, ORF58, in infecting the basolateral surfaces of polarized cells (33). The major task now is to define some of the cellular proteins that are important for MHV-68 attachment and entry and thereby to build up a comprehensive picture of how a gammaherpesvirus colonizes its natural host.

ACKNOWLEDGMENTS

This work was supported by Medical Research Council grants G108/462 and G9800903. P.G.S. is an MRC/Academy of Medical Sciences Clinician Scientist.

REFERENCES

1. **Adler, H., M. Messerle, M. Wagner, and U. H. Koszinowski.** 2000. Cloning and mutagenesis of the murine gammaherpesvirus 68 genome as an infectious bacterial artificial chromosome. J. Virol. **74:**6964–6974.
2. **Akula, S. M., N. P. Pramod, F. Z. Wang, and B. Chandran.** 2002. Integrin alpha3beta1 (CD 49c/29) is a cellular receptor for Kaposi's sarcoma-associated herpesvirus (KSHV/HHV-8) entry into the target cells. Cell **108:**407–419.
3. **Blaskovic, D., M. Stancekova, J. Svobodova, and J. Mistrikova.** 1980. Isolation of five strains of herpesviruses from two species of free living small rodents. Acta Virol. **24:**468.
4. **Boname, J. M., and P. G. Stevenson.** 2001. MHC class I ubiquitination by a viral PHD/LAP finger protein. Immunity **15:**627–636.
5. **Borza, C. M., and L. M. Hutt-Fletcher.** 1998. Epstein-Barr virus recombinant lacking expression of glycoprotein gp150 infects B cells normally but is enhanced for infection of epithelial cells. J. Virol. **72:**7577–7582.
6. **Borza, C. M., and L. M. Hutt-Fletcher.** 2002. Alternate replication in B cells and epithelial cells switches tropism of Epstein-Barr virus. Nat. Med. **8:**594–599.
7. **Brack, A. R., J. Dijkstra, H. Granzow, B. G. Klupp, and T. C. Mettenleiter.** 1999. Inhibition of virion maturation by simultaneous deletion of glycoproteins E, I, and M of pseudorabies virus. J. Virol. **73:**5364–5372.
8. **Coleman, H. M., B. de Lima, V. Morton, and P. G. Stevenson.** 2003. Murine gammaherpesvirus 68 lacking thymidine kinase shows severe attenuation of lytic cycle replication in vivo but still establishes latency. J. Virol. **77:**2410–2417.
9. **Davis-Poynter, N., S. Bell, T. Minson, and H. Browne.** 1994. Analysis of the contributions of herpes simplex virus type 1 membrane proteins to the induction of cell-cell fusion. J. Virol. **68:**7586–7590.
10. **de Lima, B. D., J. S. May, and P. G. Stevenson.** 2004. Murine gammaherpesvirus 68 lacking gp150 shows defective virion release but establishes normal latency in vivo. J. Virol. **78:**5103–5112.
11. **Dingwell, K. S., C. R. Brunetti, R. L. Hendricks, Q. Tang, M. Tang, A. J. Rainbow, and D. C. Johnson.** 1994. Herpes simplex virus glycoproteins E and I facilitate cell-to-cell spread in vivo and across junctions of cultured cells. J. Virol. **68:**834–845.
12. **Efstathiou, S., Y. M. Ho, and A. C. Minson.** 1990. Cloning and molecular characterization of the murine herpesvirus 68 genome. J. Gen. Virol. **71:**1355–1364.
13. **Flano, E., S. M. Husain, J. T. Sample, D. L. Woodland, and M. A. Blackman.** 2000. Latent murine gamma-herpesvirus infection is established in activated B cells, dendritic cells, and macrophages. J. Immunol. **165:**1074–1081.
14. **Igakura, T., J. C. Stinchcombe, P. K. Goon, G. P. Taylor, J. N. Weber, G. M. Griffiths, Y. Tanaka, M. Osame, and C. R. Bangham.** 2003. Spread of HTLV-I between lymphocytes by virus-induced polarization of the cytoskeleton. Science **299:**1713–1716.
15. **Kapadia, S. B., B. Levine, S. H. Speck, and H. W. Virgin.** 2002. Critical role of complement and viral evasion of complement in acute, persistent, and latent gamma-herpesvirus infection. Immunity **17:**143–155.
16. **Köhler, G., and C. Milstein.** 1975. Continuous cultures of fused cells secreting antibody of predefined specificity. Nature **256:**495–497.
17. **Lake, C. M., and L. M. Hutt-Fletcher.** 2000. Epstein-Barr virus that lacks glycoprotein gN is impaired in assembly and infection. J. Virol. **74:**11162–11172.
18. **Lopes, F. B., S. Colaco, J. S. May, and P. G. Stevenson.** 2004. Characterization of the MHV-68 glycoprotein B. J. Virol. **78:**13370–13375.
19. **May, J. S., H. M. Coleman, B. Smillie, S. Efstathiou, and P. G. Stevenson.** 2004. Forced lytic replication impairs host colonization by a latency-deficient mutant of murine gammaherpesvirus-68. J. Gen. Virol. **85:**137–146.
20. **May, J. S., S. Colaco, and P. G. Stevenson.** Glycoprotein M is an essential lytic replication protein of the murine gammaherpesvirus 68. J. Virol. **79:**3459–3467.

20a. **May, J. S., J. M. Boname, and P. G. Stevenson.** J. Gen. Virol., in press.

21. **Moorman, N. J., C. Y. Lin, and S. H. Speck.** 2004. Identification of candidate gammaherpesvirus 68 genes required for virus replication by signature-tagged transposon mutagenesis. J. Virol. **78:**10282–10290.
22. **Peeters, B., J. Pol, A. Gielkens, and R. Moormann.** 1993. Envelope glycoprotein gp50 of pseudorabies virus is essential for virus entry but is not required for viral spread in mice. J. Virol. **67:**170–177.
23. **Pertel, P. E.** 2002. Human herpesvirus 8 glycoprotein B (gB), gH, and gL can mediate cell fusion. J. Virol. **76:**4390–4400.
24. **Smith, G. L., B. J. Murphy, and M. Law.** 2003. Vaccinia virus motility. Annu. Rev. Microbiol. **57:**323–342.
25. **Spear, P. G., and R. Longnecker.** 2003. Herpesvirus entry: an update. J. Virol. **77:**10179–10185.
26. **Stevenson, P. G., S. Freeman, C. R. Bangham, and S. Hawke.** 1997. Virus dissemination through the brain parenchyma without immunologic control. J. Immunol. **159:**1876–1884.
27. **Stevenson, P. G., G. T. Belz, M. R. Castrucci, J. D. Altman, and P. C. Doherty.** 1999. A gamma-herpesvirus sneaks through a CD8(+) T cell re-

sponse primed to a lytic-phase epitope. Proc. Natl. Acad. Sci. USA **96:**9281–9286.

28. **Stevenson, P. G., S. Efstathiou, P. C. Doherty, and P. J. Lehner.** 2000. Inhibition of MHC class I-restricted antigen presentation by gamma 2-herpesviruses. Proc. Natl. Acad. Sci. USA **97:**8455–8460.
29. **Stevenson, P. G., J. S. May, X. G. Smith, S. Marques, H. Adler, U. H. Koszinowski, J. P. Simas, and S. Efstathiou.** 2002. K3-mediated evasion of CD8(+) T cells aids amplification of a latent gamma-herpesvirus. Nat. Immunol. **3:**733–740.
30. **Stewart, J. P., O. J. Silvia, I. M. Atkin, D. J. Hughes, B. Ebrahimi, and H. Adler.** 2004. In vivo function of a gammaherpesvirus virion glycoprotein: influence on B-cell infection and mononucleosis. J. Virol. **78:**10449–10459.
31. **Sunil-Chandra, N. P., S. Efstathiou, and A. A. Nash.** 1992. Murine gammaherpesvirus 68 establishes a latent infection in mouse B lymphocytes in vivo. J. Gen. Virol. **73:**3275–3279.
32. **Tanner, J., J. Weis, D. Fearon, Y. Whang, and E. Kieff.** 1987. Epstein-Barr virus gp350/220 binding to the B lymphocyte C3d receptor mediates adsorption, capping, and endocytosis. Cell **50:**203–213.
33. **Tugizov, S. M., J. W. Berline, and J. M. Palefsky.** 2003. Epstein-Barr virus infection of polarized tongue and nasopharyngeal epithelial cells. Nat. Med. **9:**307–314.
34. **Virgin, H. W., P. Latreille, P. Wamsley, K. Hallsworth, K. E. Weck, A. J. Dal Canto, and S. H. Speck.** 1997. Complete sequence and genomic analysis of murine gammaherpesvirus 68. J. Virol. **71:**5894–5904.
35. **Weck, K. E., S. S. Kim, H. W. Virgin, and S. H. Speck.** 1999. Macrophages are the major reservoir of latent murine gammaherpesvirus 68 in peritoneal cells. J. Virol. **73:**3273–3283.